communications in mathematical
match
and in computer chemistry

no. 47, January 2003
MATCDY (47) 53- 70 (2003)

ISSN 0340 - 6253

Azulenic Tori

Mircea V. Diudea,[1,*] Basil Pârv[2] and Edward C. Kirby[3]

[1]Babeş-Bolyai University, Faculty of Chemistry and Chemical Engineering
Babes-Bolyai University, 3400 Cluj, ROMANIA

[2]Babeş-Bolyai University, Faculty of Mathematics and Computer Science,
Department of Computer Science, Babes-Bolyai University, 3400 Cluj, ROMANIA

[3]Resource Use Institute, 14 Lower Oakfield, Pitlochry,
Perthshire PH16 5DS, Scotland, UK.

(Received September 26, 2002)

Abstract. Tubular nanostructures are cylindrical trigonally hybridized carbon atom networks, obtained from the vaporized graphite. They are usually tessellated entirely by hexagons and show unusual properties (electronic, optical, mechanical, etc.). Several utilizations in "nanoscale" devices have already been proposed. Toroidal models were proposed in connection with the observed circular "ropes". Pentagons and heptagons are involved in some observed defects or designed with a view to relief of strain in tightly curved tubules or tori. Pentaheptite nets are well-known in the boron chemistry. In this paper, a novel method for generating pentaheptite (*i.e.*, azulenic) tori, based on appropriate cutting performed on a square lattice embedded on the toroidal surface, is presented. These structures are investigated for structural stability by molecular mechanics MM+ procedure. Spectral data are calculated at the simple π-electron Hückel level. They indicate that the pentaheptite objects are closed or at most open shells, in contrast to the earlier reported metallic behavior. Extended Hückel

* Correspondence author; phone: 00-40-264-412-106; fax: 00-40-264-190-818;
E-mail: diudea@chem.ubbcluj.ro

theory EHT data providing (with some exceptions) non-zero band gaps, support the above finding. Topological characterization, by the spiral code, is also given.

INTRODUCTION

Novel pure carbon nanostructures have excited the interest of the scientists during the last two decades.[1-11] Besides the classical spherical fullerenes, (tiled with pentagons and hexagons) pure graphitic polyhex cylinders [12-14] and toroids [15-37] have been obtained or proposed to account for the observed coiled ropes. [15-17]

As an alternative to the graphitic structures, pentaheptite tessellations with various local signatures have been proposed. [38,39] Such structures appear in the boron chemistry and it was suggested that pure pentaheptite carbon nets could have metallic character. [40] Rings of size C_5 and C_7 were also used for curvature matching and strain relief in otherwise all-hexagon small tori. [19, 22, 37, 41]

A pentaheptite net can be drawn by means of the Stone-Wales transformation of a hexagonal net. [39, 42] Our method used here proceeds by appropriate modification of an all-C_4 square-like tiling [43-47] (Figure 1). The resulting C_5C_7 net shows a local (t_5, t_7) signature of (1,3) type.

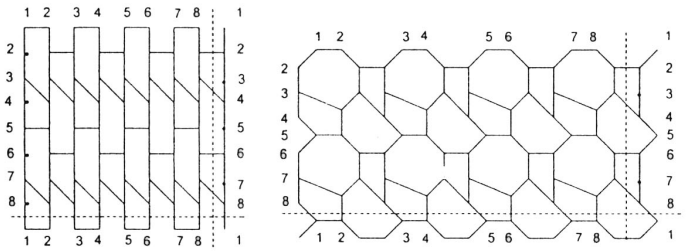

Figure 1. A C_5C_7 azulenic net derived from an all-C_4 lattice.

The cutting procedure can involve either horizontal or vertical edges in the parent square net. The name of the resulting objects is a string of alphanumeric characters indicating the edge-cutting type, and size of the tiling polygons. The object dimensions (in square

brackets) follow the letters and represent: c - the number of atoms on the c-gonal tube cross section and n - the number of copies of the c-gon around the torus hole. Thus, HC5C7 [8,24] reads: horizontal pentaheptite of tube size 8 and torus dimension 24.

In HC_5C_7 [c,n] tori, each C_5C_7 pair takes exactly four squares in the parent net, so that $c/4$ such pairs lie around the tube. The n-dimension is, in this case, preserved. Conversely, in VC_5C- [c,n] tori, the constant dimension is c, while $n/4$ equals the number of pairs around the torus (see Figure 2). Note that, the [c,n] dimensions are just the dimensions of the parent all-C_4 lattice, that remain unchanged by the cutting operations. The number of atoms is given by the product c x n.

TOROIDAL STRUCTURES

A pentaheptite net induces a twisting particularly in toroidal structures. As a consequence, only very thin tori could be optimized to a plausible geometry. Thin tubes are have been observed or modeled. [28] Two isomeric tori C_5C_7 [8,44] are illustrated in Figure 2.

HC_5C_7 [8,44] (side)
8 x 44 = 352 atoms; 2 x 44 = 88 C_5C_7 pairs

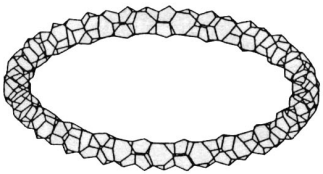

HC_5C_7 [8,44] (top)

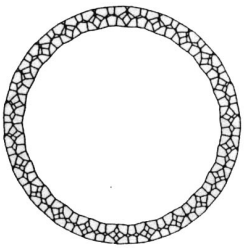

Figure 2. Two isomeric tori C_5C_7 [8,44]

VC_5C_7 [8,44] (side)
8 x 11 = 88 C_5C_7 pairs

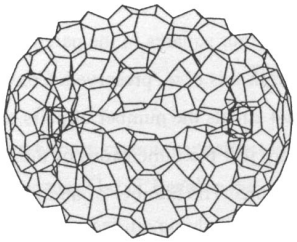

VC_5C_7 [8,44] (top)

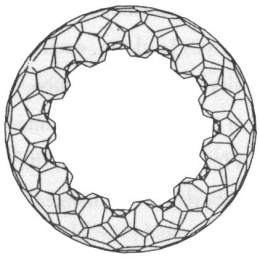

Figure 2. (continued)

Buckling appears on thicker tubed tori, as shown in the case of optimized VC_5C_7 [8,44] (Figure 2). Attempts to optimize larger tube tori lec to very unrealistic objects, clearly deviating badly from a toroidal surface that is everywhere locally planar (Figure 3). Their molecular mechanics MM+ energies (in kcal/mol) [48] are higher than those of the thin objects included in Table 1 (see below).

HC_5C_7 [20,64]; MM+ = 11399.296

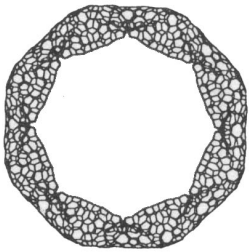

HC_5C_7 [20,96]; MM+ = 16665.922

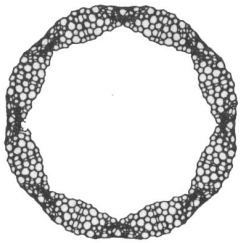

Figure 3. Two distorted tori obtained as a result of optimizing relatively thick tubes.

OPEN STRUCTURES

An open tube can be obtained by appropriate cutting of a torus. After a molecular mechanics optimization, a nice tube with azulenic tessellation is obtained. The two ends are different: one is crenellated and the other one is zigzag (see Figure 4). The isomeric tubes of $TUHC_5C_7$ [20,100] have 2000 atoms and, respectively, 495 and 480 C_5C_7 pairs. Note that, the naming of tori was previously established, [43-47] so that the name of a spanning tube is made by adding the letters "TU" at the beginning of the string naming the corresponding torus.

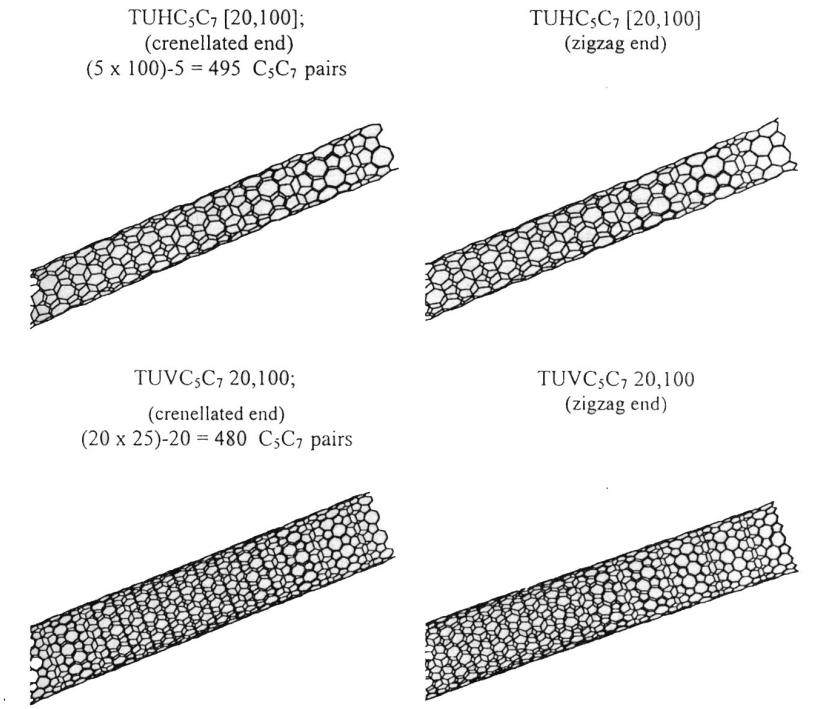

Figure 4. Two isomeric open azulenic tubes.

MOLECULAR MECHANICS CALCULATION

Molecular mechanics calculations have been performed, by MM+ force field of Hyper-Chem [48] (Hypercube, Inc.), at 0.01 rms.

Thin Tubes

Table 1 lists the values of total MM+ energy per atom (in kcal·mol^{-1}) for tori and corresponding open tubes. Also given is the strain energy, defined as the difference in energy per atom between them. We have taken torus [8,20] as the lower limit, where the structure strain shows a pertinent relief.

Table 1. MM+ (0.01 rms; kcal·mol^{-1}) and EHT (a.u.) Energy for the HC_5C_7 [8,*n*] Tubes. Strain Energy SE (kcal/mol) for Tori is also Given.

n	Tube		Torus		
	MM+ / atom	EHT / atom	MM+ / atom	SE / atom	EHT / atom
20	12.499	-2.54306	24.700	12.200	-2.50286
22	12.558	-2.54307	24.063	11.505	-2.50374
24	12.607	-2.54306	23.589	10.982	-2.50454
26	12.649	-2.54306	23.230	10.581	-2.50530
28	12.684	-2.54305	22.951	10.267	-2.50601
30	12.715	-2.54305	22.731	10.016	-2.50668
32	12.742	-2.54305	22.554	9.812	-2.50729
34	12.766	-2.54306	22.410	9.644	-2.50788
36	12.787	-2.54305	22.291	9.504	-2.50841
38	12.806	-2.54305	22.192	9.386	-2.50892
40	12.823	-2.54304	22.109	9.286	-2.50940
42	12.838	-2.54304	22.038	9.200	-2.50986
44	12.852	-2.54305	21.977	9.125	-2.51022
46	12.865	-2.54306	21.924	9.059	-2.51055
48	12.877	-2.54305	21.879	9.002	-2.51098
50	12.887	-2.54305	21.839	8.951	-2.51127
52	12.897	-2.54305	21.803	8.906	-2.51157
54	12.907	-2.54304	21.772	8.866	-2.51181
56	12.915	-2.54304	21.745	8.829	-2.51207
58	12.923	-2.54304	21.720	8.797	-2.51231
60	12.931	-2.54304	21.698	8.767	-2.51255
62	12.938	-2.54304	21.678	8.740	-2.51276
64	12.944	-2.54304	21.660	8.715	-2.51294
66	12.951	-2.54304	21.643	8.693	-2.51314

Table 1. (continued)

68	12.956	-2.54304	21.628	8.672	-2.51328
70	12.961	-2.54304	21.615	8.653	-2.51342
72	12.967	-2.54303	21.602	8.636	-2.51358
74	12.971	-2.54303	21.591	8.619	-2.51372
76	12.976	-2.54303	21.581	8.604	-2.51384
78	12.981	-2.54303	21.571	8.590	-2.51398
80	12.985	-2.54302	21.562	8.577	-2.51409
82	12.989	-2.54303	21.554	8.564	-2.51420
84	12.992	-2.54303	21.546	8.554	-2.51429
86	12.996	-2.54303	21.539	8.543	-2.51440
88	13.000	-2.54302	21.533	8.533	-2.51450
90	13.003	-2.54304	21.526	8.524	-2.51457
92	13.006	-2.54303	21.521	8.515	-2.51467
94	13.009	-2.54303	21.515	8.507	-2.51473
96	13.012	-2.54302	21.510	8.499	-2.51485
98	13.014	-2.54303	21.506	8.491	-2.51489
100	13.018	-2.54304	21.501	8.484	-2.51501

The MM+ energy per atom shows a positive dependency on n, which tends towards linearity with increasing n, for both open and toroidal tubes, although always with higher values for the latter (Figure 5). The torus strain energy per atom (Table 1, and shown as the difference between pairs of points in Figure 5), behaves similarly but gradually reduces in magnitude.

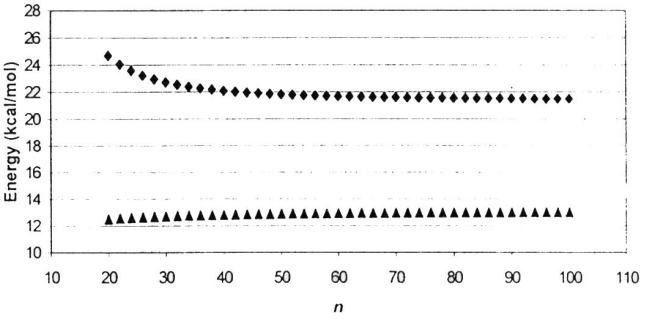

Figure 5. Plot of MM+ energy per atom *vs.* n for tori HC_5C_7 [8,n] (top) and tubes $TUHC_5C_7$ [8,n] (bottom); the difference between pairs of points represents strain energy (see Table 1)

We compared the thin torus HC_5C_7 [8,100] to the corresponding HC_6 [8,100] (polyhex) and HC_4C_8 [8,100] (bathroom floor) tiled tori (Table 2). It can be seen that the strain energy per atom of HC_5C_7 [8,100] is far higher than the others. For comparison, the V-tori, where they are stable, are included. Further images illustrating these thin tori (which optimize well) are shown in Figure 6.

Table 2. MM+ Energy/atom (at 0.01 rms) of [8,100] Objects

No	Lattice	H-Torus	H-Tube	Strain Energy	V-Torus	V-Tube	Strain Energy
1	C_6	11.451	10.949	0.501	6.270	3.697	2.572
2	C_4C_8	16.556	16.235	0.322	13.764	11.632	2.131
3	C_5C_7	21.501	13.018	8.484	-	5.373	-

HC_6 [8,100] (side)

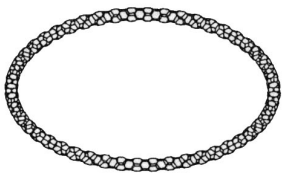

HC_4C_8 [8,100] (side)

Figure 6. Further examples of optim.zed thin tori

Thick Tubes

In the foregoing sections we have examined the effect of varying the *length* of an azulenic tube. We now consider its *width*, by taking tubes $TUHC_5C_7$ [c,100] and $TUVC_5C_7$ [c,100], for increasing c-values in the range (8, 32) (see Table 3).

Table 3. Total MM+ Energy/atom (kcal/mol) for Tubes TUC_5C_7 [c,100]

No	c	$TUHC_5C_7$	$TUVC_5C_7$
1	8	13.018	5.373
2	12	7.843	3.264
3	16	5.424	2.410
4	20	4.099	1.990
5	24	3.301	1.754
6	28	2.788	1.610
7	32	2.441	1.515

The total energy per atom shows a power law function of the c-dimension, as shown in Figure 7. As the tube cross-section increases, the structures become more relaxed (and thus more stable). Note that the total MM+ energy mainly accounts for the constitutional stability, involving the contribution of the σ-bonds rather than to that of π-bonds.

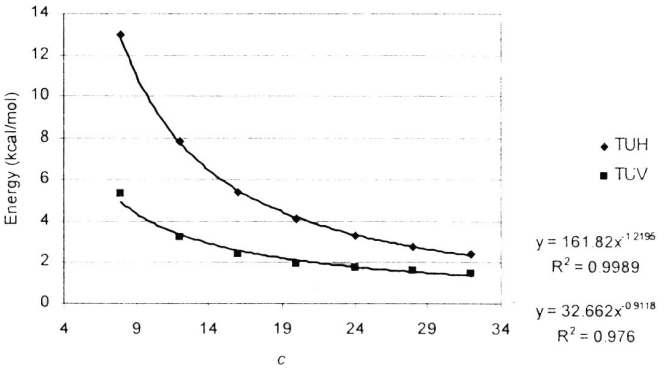

Figure 7. Plot of total MM+ energy per atom *vs.* the c-dimension in thick tubes TUC_5C_7 [c,100]

ELECTRONIC STRUCTURE

In the π-only Hückel theory, the energy of the i^{th} molecular orbital is written as:

$$E_i = \alpha + \lambda_i \beta$$

where λ_i are the eigenvalues of the adjacency matrix of the corresponding molecular graph.

Theoretical calculations, performed so far [34, 36, 49], predict for the graphitic single-walled carbon nanotubes and their corresponding toroids either metallic or semiconducting behavior depending only on their diameter and helicity. Criteria for the metallic and insulating character of nanotubes were established in terms of the graphite-zone folding building procedure.

The metallic character involves the existence of a zero bandgap (*i.e.*, BANDGAP = E_LUMO - E_HOMO) and the degeneracy of some non-bonding orbitals [49] (NBOs) favoring the spin multiplicity, cf. the Hund rule. In polyhex tori, the metallic behavior is ensured by *four* NBOs, also present in the graphite sheet and in C_{20}.

As for azulene itself, in all the azulenic objects tested here, the spectra show no mirror symmetry about $\lambda = 0$, as a consequence of their non-alternant structures with odd-membered cycles. Only two cases were observed:

(a) *Open-shell*, with $\lambda_{N/2} = \lambda_{N/2+1} > 0$ (implying a zero bandgap, see Table 4) and $n/2$ degenerate orbitals at $\lambda_{N/2}$ value, for tori of series HC_5C_7 [8,*n*]. In case of VC_5C_7 [8,*n*] series or in tori having $c > 8$ the degenerate orbitals appear at $\lambda_{N/2-p}$, p>1.

(b) *Pseudo closed-shell*, with $\lambda_{N/2} > \lambda_{N/2+1} \geq 0$ (with a non-zero bandgap) and $n/2$-1 degenerate orbitals at $\lambda_{N/2-1}$ value, for tubes of series $TUHC_5C_7$ [8,*n*].

HMO bandgap results are included in Table 4. Figure 8 illustrates the trend (towards zero at n equal to infinity) of the bandgap as n increases, for the open tubes of series HC_5C_7 [8,*n*].

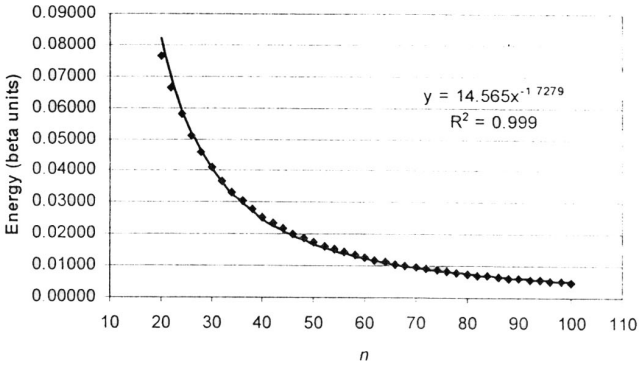

Figure 8. The HMO bandgap in open tubes of series HC_5C_7 [8,*n*].

With the aim of providing additional support for the above shell structure, extended Hűckel calculations were performed (by EHT procedure of Hyper-Chem program, version 4.0, with an unweighted Huckel Constant = 1.75, on molecular structures optimized by the MM+ procedure, at 0.01 rms.).

Table 1 includes the EHT energy per atom for the series HC_5C_7 [8,*n*]. The structures have been optimized by MM+ calculation at rms lower than 0.01. The energy is almost constant for tubes while in tori it decreases as *n* increases (Figure 9), indicating an energetic relaxation of the objects, consistent with the expectation that strain should reduce as the large radius of the torus increases.

Values of the EHT bandgap for the series HC_5C_7 [8,*n*] are given in Table 4. A plot of the bandgap against *n* ($n > 40$) , for these tori is shown in Figure 10.

As can be seen from table 4, only four clean zero values are observed, while most of them are quite different from zero. However, a difference between HMO and EHT data is expected, since the EHT data are geometry dependent (in addition to the consideration of sp_2 and $2p_z$ atomic orbitals) while HMO ones are not. As mentioned above, the pattern C5C7 induces a twisting of the whole structure, particularly in tori with a large central hollow. The open tubes show non-zero band gap in both of the two approaches.

Table 4. Bandgap Provided by HMO (β units) and EHT (eV) Calculation for Azulenic Objects of Series HC_5C_7 [8,*n*]

n	HMO		EHT	
	Tori	Tubes	Tori	Tubes
20	0	0.07624	0	0.03019
22	0	0.06622	0.06834	0.03895
24	0	0.05806	0	0.01619
26	0	0.05132	0	0.02781
28	0	0.04569	0.04809	0.02377
30	0	0.04094	0.03796	0.01754
32	0	0.03689	0	0.01783
34	0	0.03341	0.04071	0.02269
36	0	0.03040	0.05629	0.00995
38	0	0.02778	0.13857	0.01751
40	0	0.02549	0.19734	0.01567
42	0	0.02346	0.20515	0.01134
44	0	0.02167	0.20461	0.01221
46	0	0.02007	0.19607	0.01565
48	0	0.01864	0.18231	0.00705
50	0	0.01736	0.16704	0.01198
52	0	0.01621	0.14945	0.01159
54	0	0.01517	0.13268	0.00806
56	0	0.01422	0.11730	0.00939
58	0	0.01336	0.10260	0.01192
60	0	0.01257	0.09029	0.00560
62	0	0.01186	0.08054	0.00955
64	0	0.01120	0.07302	0.00938
66	0	0.01059	0.05762	0.00686
68	0	0.01003	0.04408	0.00662
70	0	0.00952	0.03414	0.00997
72	0	0.00904	0.02719	0.00463
74	0	0.00860	0.02053	0.00731
76	0	0.00819	0.00507	0.00777
78	0	0.00781	0.02045	0.00583
80	0	0.00745	0.02183	0.00551
82	0	0.00712	0.02423	0.00835
84	0	0.00681	0.02963	0.00416
86	0	0.00652	0.03919	0.00622
88	0	0.00625	0.04465	0.00672
90	0	0.00599	0.04595	0.00475
92	0	0.00575	0.05059	0.00453
94	0	0.00553	0.05700	0.00716
96	0	0.00531	0.06187	0.00375
98	0	0.00511	0.06518	0.00521
100	0	0.00492	0.06950	0.00590

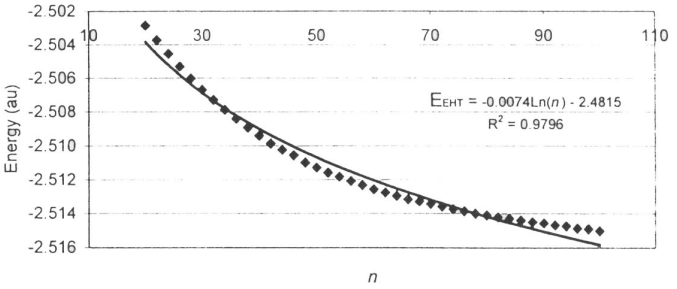

Figure 9. Energy (EHT) per atom *vs.* the *n*-dimension of tori.

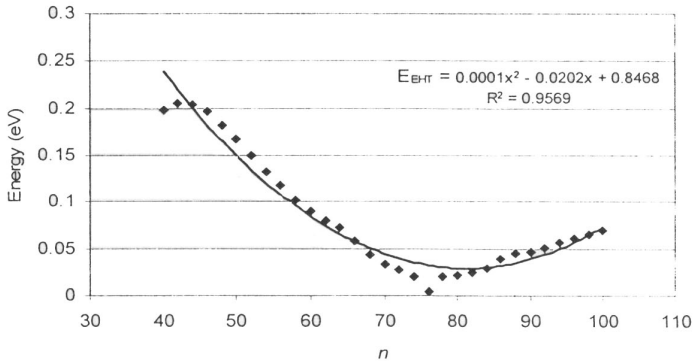

Figure 10. The trend of the energy gap in tori of series HC_5C_7 [8,*n*] at $n > 40$.

No metallic character is envisaged by our tubular structures (consisting of a pentaheptite net with the local (t_5, t_7) signature of (1,3), in hard contradiction with the previous suggestion of Crespi *et al.* [40]. In addition, the azulenic sheet is clearly a pseudo closed-shell. However, the bandgap is very close to zero, suggesting a kinetic instability of these molecules. For comparison, C_{60} -a properly closed shell structure shows an energy gap value of 1.433 eV. The high degeneracy of some levels close to the HOMO orbital, in pentaheptite tori, could be taken into account in defining the character of the MO levels. The

molecule azulene (C_5C_7) has a $4n + 2$, $n = 2$ periphery and under reacting conditions can form two complementary charged π-electron aromatic sextets [50-53], by charge transfer. (This is often used to account for the fact that azulene is, in general, much more reactive than its isomer naphthalene.) In the case of two abutting pentagons (*i.e.*, pentalene) however, the total contour is an eight-membered one, which is not favorable to the aromatic character. Moreover, the presence of charges of the same sign in two adjacent pentagons (or heptagons) would destabilize further an odd-membered cycle non-alternating net.

At this point it is appropriate to reflect on the terminology being used. In this paper, and in the original proposal for toroidal azulenoids [38], these (1,3) pentaheptite nets are referred to as azulenoid or azulenic because they amount to tiling a surface with azulene alone. However, while such a surface may be completely *tiled* with azulenes, it is not *fully* azulenoid in the sense that Kirby [54] later suggested. It is not possible to formulate the net as a set of azulenes connected by essentially single bonds (by analogy with the fully sextet benzenoids of Clar [50]), or in graph theoretical language it does not have a 2-factor consisting of a set of disconnected azulene subgraphs. To achieve that, other sized rings must be introduced.[54] On the other hand these pentaheptite nets, when in closed toroidal form, *can* be perceived as being fully pentalenic, so that the character of pentalene is possibly more relevant than azulene to their properties.

Encoding the type of tessellation can also be achieved by means of the spiral code. It was first proposed for coding and constructing spherical fullerenes [55, 56]. Diudea [57] proposed recently a modification, useful in tubular structures. In a periodic tubular net, the spiral code brings information on size and sequence of faces and embedding the actual net on the parent all-C_4 $[c,n]$. The spiral code for the azulenic toroidal nets is as follows:

$$S(HC_5C_7) = \left[(5\ 7)_{c/4}, (7\ 5)_{c/4}\right]_{(n/4)}$$

$$S(VC_5C_7) = \left[(5\ 7)_{c/2}, (7\ 5)_{c/2}\right]_{(n/8)}$$

CONCLUSIONS

A number of smaller all-azulene, *i.e.*, pentaheptite, tubes and tori have been modeled, and the results suggest that, although they are likely to have higher energy than their polyhex or C4C8 counterparts, at least some of them are capable of stable existence. A pentaheptite network induces significant twisting, which tends to cause a tube to bend by buckling rather than with a smooth curvature, and azulenoid tori with tube circumference larger than eight atoms (equivalent to four C5C7 pairs in H-tori and eight pairs in V-tori) could not be optimized with the tube lengths employed. Spectral and EHT data reported here give a negative answer to Crespi *et al.*, which predicted a metallic behavior for the pentaheptite net. Further studies are needed to fully define the set of optimizable structures.

ACKNOWLEDGEMENTS. This work is supported, in part, by Romanian CNCSIS Grant, 2002. The authors acknowledge the referees' help in improving this paper.

REFERENCES

[1] H. W. Kroto, J. R. Heath, S. C. O'Brien, R. F. Curl, and R. E. Smalley, C_{60} – Buckminsterfullerene, *Nature* **1985**, *318*, 162-163.

[2] P. W. Fowler and D. E. Manolopoulos, *An Atlas of Fullerenes*, Oxford University Press, Oxford, 1995.

[3] A. J. Stone and D. J. Wales, Theoretical studies of icosahedral C_{60} and some related species, *Chem. Phys. Lett.* **1986**, *128*, 501-503.

[4] T.G. Schmalz, W.A. Seitz, D.J. Klein, and G.E. Hite, Elemental carbon cages, *J. Am. Chem. Soc.* **1988,** *110*, 1113-1127.

[5] H. Kroto, The first predictions in the buckminsterfullerene crystal ball, *Fullerene Sci. Technol.* **1994**. *2*, 333-342.

[6] F. Diedrich and C. Thilgen, Covalent fullerene chemistry, *Science* **1996**, *271*, 317-323.

[7] D. E. Cliffel and A. J. Bard, Electrochemistry of tert-butylcalix[8]arene-C60. Films using a scanning electrochemical microscope-quartz crystal microbalance, *Anal. Chem.* **1998**, *70*, 4146-4151.

[8] J. Liu, J. Alvarez, W. Ong, and A. E. Kaifer, Network aggregates formed by C60 and gold nanoparticles capped with a-cyclodextrin hosts, *Nano Lett.* **2001**, *1*, 57-60.

[9] N. Tagmatarchis and H. Shinohara, Production, separation, isolation, and spectroscopic study of dysprosium endohedral metallofullerenes, *Chem. Mater.* **2000**, *12*, 3222-3226.

[10] N. Tagmatarchis, E. Aslanis, K. Prassides, and H. Shinohara, Mono-, di- and trierbium endohedral metallofullerenes: production, separation, isolation, and spectroscopic study, *Chem. Mater.* **2001**, *13*, 2374-2379.

[11] T. Da Ros, G. Spalluto, and M. Prato, Biological applications of fullerene derivatives: a brief overview, *Croat. Chem. Acta* **2001**, *74*, 743-755.

[12] S. Iijima, Helical microtubules of graphitic carbon, *Nature* **1991**, *354*, 56-58.

[13] S. Iijima and T. Ichihashi, Single-shell carbon nanotubes of 1 nm diameter, *Nature* 1993, *361*, 603-605.

[14] A. L. Ivanovskii, Simulation of nanotubular forms of matter, *Russ. Chem. Rev.* **1999**, *68*, 103-118.

[15] J. Liu, H. Dai, J. H. Hafner, D. T. Colbert, R. E. Smalley, S. J. Tans, and C. Dekker, Fullerene crop circles, *Nature* **1997**, *385*, 780-781.

[16] R. Martel, H. R. Shea, and P. Avouris, Rings of single-walled carbon nanotubes, *Nature* **1999**, *398*, 299-299.

[17] R. Martel, H. R. Shea, and P. Avouris, Ring formation in single-wall carbon nanotubes, *J. Phys. Chem. B*, **1999**, *103*, 7551-7556.

[18] M. Ahlskog, E. Seynaeve, R. J. M. Vullers, C. Van Haesendonck, A. Fonseca, K. Hernadi, and J. B. Nagy, Ring formation from catalytically synthesized carbon Nanotubes, *Chem. Phys. Lett.* **1999**, *300*, 202-206.

[19] S. Itoh and S. Ihara, Toroidal form of carbon C_{360}, *Phys. Rev., B* **1993**, *47*, 1703-1704.

[20] S. Ihara and S. Itoh, Toroidal forms of graphitic carbon, *Phys. Rev., B* **1993**, *47*, 12908-12911.

[21] S. Itoh, S. Ihara, and J. Kitakami, The tori can be derived from tubules (8,2), *Phys. Rev., B* **1993**, *47*, 1703.

[22] S. Itoh and S. Ihara, Toroidal forms of graphitic carbon. II. Elongated tori, *Phys. Rev., B* **1993**, *48*, 8323-8328.

[23] S. Itoh and S. Ihara, Isomers of the toroidal forms of graphitic carbon, *Phys. Rev., B* **1994**, *49*, 13970-13974.

[24] J. K. Johnson, B. N. Davidson, M. R. Pederson, and J. Q. Broughton, Energetics and structure of toroidal forms of carbon, *Phys. Rev., B* **1994**, *50*, 17575-17582.

[25] B. Borstnik and D. Lukman, Molecular mechanics of toroidal carbon molecules, *Chem. Phys. Lett.* **1994**, *228*, 312-316.

[26] J. E. Avron and J. Berger, Tiling rules for toroidal molecules, *Phys. Rev., A* **1995**, *51*, 1146-1149

[27] V. Meunier, P. Lambin, and A. A. Lucas, Atomic and electronic structures of large and small carbon tori, *Phys. Rev., B* **1998**, *57*, 14886-14890.

[28] D-H. Oh, J. M. Park, and K. S. Kim, Structures and electronic properties of small carbon nanotube tori, *Phys. Rev., B* **2000**, *62*, 1600-1603.

[29] M. F. Lin and D. S. Chuu, Persistent currents in toroidal carbon nanotubes, *Phys. Rev. B* **1998**, *57*, 6731- 6737.

[30] A. Ceulemans, L. F. Chibotaru, and P. W. Fowler, Molecular anapole moments, *Phys. Rev. Lett.* **1998**, *80*, 1861-1864.

[31] E. C. Kirby and T. Pisanski, Aspects of topology, genus and isomerism in closed 3-valent networks, *J. Math. Chem.* **1998**, *23*, 151-167.

[32] E. C. Kirby, Cylindrical and toroidal polyhex structures, *Croat. Chem. Acta* **1993**, *66*, 13-26.

[33] E. C. Kirby, R. B. Mallion, and P. Pollak, Toroidal polyhexes, *J. Chem. Soc. Faraday Trans.* **1993**, *89*, 1945-1953.

[34] A. Ceulemans, L. F. Chibotaru, S. A. Bovin, and P. W. Fowler, The electronic structure of polyhex carbon tori, *J. Chem. Phys.* **2000**, *112*, 4271-4278.

[35] D. Marušić and T. Pisanski, Symmetries of hexagonal molecular graphs on the torus, *Croat. Chem. Acta* **2000**, *73*, 969-981.

[36] S. A. Bovin, L. F. Chibotaru, and A. Ceulemans, The quantum structure of carbon tori, *J. Mol. Catalysis, A* **2001**, *166*, 47-52.

[37] D. Babić, D. J. Klein, and T. G. Schmalz, Curvature matching and strain relief in bucky-tori: usage of sp^3-hybridization and nonhexagonal rings, *J. Mol. Graphics Modell.* **2001**, *19*, 222-231.

[38] E. C. Kirby, On toroidal azulenoids and other shapes of fullerene cage, *Fullerene Sci. Technol.* **1994**, *2*, 395-404.

[39] M. Deza, P. W. Fowler, M. Shtogrin, and K. Vietze, Pentaheptite modifications of the graphite sheet, *J. Chem. Inf. Comput. Sci.* **2000**, *40*, 1325-1332

[40] V. H. Crespi, L. X. Benedict, M. L. Cohen, and S. G. Louie, Prediction of a pure-carbon covalent metal, *Phys. Rev. B* **1996**, *53*, 13303-13305.

[41] S. Iijima, T. Ichihashi, and Y. Ando, Pentagons, heptagons and negative curvature in graphite microtubule growth, *Nature* **1992**, *356*, 776-778.

[42] Z. Yao, H. W. C. Postma, L. Balents, and C. Dekker, Carbon nanotube intramolecular junctions, *Nature* **1999**, *402*, 253-254.

[43] M. V. Diudea, I. Silaghi-Dumitrescu, and B. Parv, Toranes versus torenes, *MATCH - Commun. Math. Comput. Chem.* **2001**, *44*, 117-133.

[44] M. V. Diudea and E. C. Kirby, The energetic stability of tori and single-wall tubes, *Fullerene Sci. Technol.* **2001**, *9*, 445-465.

[45] M. V. Diudea and P. E. John, Covering polyhedral tori, *MATCH - Commun. Math. Comput. Chem.* **2001**, *44*, 103-116.

[46] M. V. Diudea, Graphenes from 4-valent tori, *Bull. Chem. Soc. Japan* **2002**, *75*, 487-492.

[47] M. V. Diudea, I. Silaghi–Dumitrescu, and B. Pârv, Toroidal fullerenes from square tiled tori, *Internet Electron. J. Mol. Des.* **2002**, *1*, 10–22, http://www.biochempress.com.

[48] HyperChem [TM], release 4.5 for SGI, © 1991-1995, Hypercube, Inc.

[49] M. Yoshida, M. Fujita, P. W. Fowler, and E. C. Kirby, Non-bonding orbitals in graphite, carbon tubules, toroids and fullerenes, *J. Chem. Soc., Faraday Trans.* **1997**, *93*, 1037-1043.

[50] E. Clar, *The Aromatic Sextet*, Wiley, New York, 1972.

[51] D. J. Klein, Aromaticity *via* Kekulé structures and conjugated circuits, *J. Chem. Ed.* **1992**, *69*, 691-694.

[52] O. Ivanciuc, L. Bytautas, and D. J. Klein. Mean–field resonating–valence–bond theory for unpaired π–electrons in benzenoid carbon species, *J. Chem. Phys.* **2002**, 116, 4735–4748

[53] J. Aihara and M. Hirama, There are no antiaromatic molecules in interstellar space, *Internet Electron. J. Mol. Des.* **2002**, *1*, 52–58, http://www.biochempress.com.

[54] E.C. Kirby, Fully arenoid toroidal fullerenes, both benzenoid and non-benzenoid, *MATCH - Commun. Math. Comput. Chem.* **1996**, 33, 147-156.

[55] G. Brinkmann and A. W. M. Dress, A constructive enumeration of fullerenes, *J. Algorithms* **1997**, *23*, 345-358.

[56] P. W. Fowler, T. Pisanski, A. Graovac, and J. Žerovnik, A generalized ring spiral algorithm for coding fullerenes and other cubic polyhedra, *DIMACS Ser. Discrete Maths. Theor. Comput. Sci.* **2000**, *51*, 175-187.

[57] M. V. Diudea, Topology of naphthylenic tori, *Phys. Chem. Chem. Phys.* **2002**, *4*, 4740-4746.